https://doi.org/10.46813/2026-161-155

MODELING THE EARLY STAGE OF THE PHENOMENON OF RADIATION GROWTH OF ZIRCONIUM

O.G. Trotsenko, P.M. Ostapchuk
Institute of Electrophysics and Radiation Technologies of the NAS of Ukraine, Kharkiv, Ukraine
E-mail: oleg-trotsenko@ukr.net

The Cluster Dynamics method was used to describe the early stage of "irradiation growth" of a zirconium single crystal, allowing for the description of its microstructure evolution with the irradiation dose. The results of numerical calculations of the dependence of point defects concentration on the dose in the absence of thermal emission, the dependence of the growth deformation along the main axes of a single crystal $\langle a \rangle$, $\langle c \rangle$ and the dependence of interstitial and vacancy loop concentrations of on their radii for doses up to 1 dpa and various diffusion coefficients of point defects are given.

PACS: 62.20Dc; 62.20.Fc

INTRODUCTION

Irradiation growth (IG) phenomenon is radiation-induced anisotropic deformation (RIAD) without an external stress and without a noticeable change in the volume of the material (as opposed to swelling). It is inherent in hcp-metals, in particular, zirconium – the structural material of fuel cell shells. This irradiation growth is related to the elimination of point defects on the different sinks (dislocations lines, surfaces, grain boundaries) and also to their agglomeration in the form of dislocation loops. But in zirconium and its alloys, some aspects of dislocation loop microstructure evolution under irradiation are rather unusual compared to cubic metals, such as the growth of vacancy loops [1–4].

The main theoretical concept of explaining most RIAD phenomena is related to the assumption that different sinks for point defects (PD), vacancies and self – interstitial atoms (SIA) absorb them differently [5, 6]. In the theory, a so-called preference factor appears $B = \frac{Z_i - Z_v}{Z_i}$ for the absorption of PD by the sink of this type. If $B > 0$, the sink absorbs more interstitial atoms, if $B < 0$ – more vacancies. As a result, different sinks evolve differently, the initial optimal microstructure of the material changes, the material is deformed. And this, as a rule, is unacceptable. In particular, zirconium single crystal expands in the $\langle a \rangle$-direction and shrinks along the $\langle c \rangle$-axe during the process of irradiation growth. This behavior is associated with the evolution of so-called $\langle a \rangle$-, $\langle c \rangle$-loops. The prismatic loops or $\langle a \rangle$-loops: they have a $\vec{b} = 1/3\langle 11\bar{2}0 \rangle$ Bürgers vector (parallel to the $\langle a \rangle$-axis of the lattice structure). They are lying approximately in the prismatic planes $(10\bar{1}0)$. In certain situations, both vacancy and interstitial loops can coexist. The basal loops or $\langle c \rangle$-loops: they are lying in the (0001) plane and their Bürgers vector has a component along the $\langle c \rangle$-axis. These loops are almost always vacancy type. They can be perfect loops ($\vec{b} = \langle 0\,0\,0\,1 \rangle$) or imperfect loops ($\vec{b} = 1/2\langle 0\,0\,0\,1 \rangle$). During neutron irradiation $\langle a \rangle$-loops form first, $\langle c \rangle$-loops formation is observed only above a certain fluence ($\sim 2\ldots3$ dpa). It is this early stage that interests us at the first stage of research. Regarding the physical explanation of this fact, two options are currently being considered: elastic interaction of PD with zirconium dislocations and diffusion anisotropy of PD between its planes. The fact is that the values $Z_{i,v}$ of PD absorption efficiency (i – interstitial atoms, v – vacancies) are determined from the solution of the corresponding diffusion problem of PD absorption by a specific sink, taking into account either the elastic interaction between them, or the anisotropic diffusion of PD. That is, the physical mechanism of absorption is "laid" precisely in $Z_{i,v}$. And then numerical calculations using the method of cluster dynamics. The goal is to compare the role of both mechanisms and, in the future, to combine them in the theory of IG of zirconium.

EQUATIONS SYSTEM

According to [7], the relative deformation ε_a along the $\langle a \rangle$-axis is given by the formula

$$\varepsilon_a = 1/2\,\omega\, Q_i^a \approx 1/2\,\omega\,(C_v - C_i), \qquad (1)$$

where Q_i^a is the net quantity of SIA in the $\langle a \rangle$-loops expressed per unit volume; ω is the atomic volume; $C_{v,i}$ is the number of vacancies (v) and SIA (i) per unit volume of the crystal. A "large" annealed single crystal of zirconium is considered, therefore absorption by grain boundaries is not taken into account. The relative strain ε_c along the $\langle c \rangle$-axis has the form [7]:

$$\varepsilon_c = -\omega\, C_v\, V_v^{rel}. \qquad (2)$$

Since there are no vacancy loops in the base plane at the early stage of irradiation, it is assumed that the deformation occurs due to the relaxation of vacancies.

The relaxation volume is taken according to [8] $V_v^{rel} = 0.43$. Calculations of the evolution over time of PD concentrations $C_{v,i}$, as well as their clusters $C_{jv,i}$, were carried out by the method of cluster dynamics [9]. For PD concentrations we have:

$$\frac{dC_v}{dt} = (K/\omega) - K_1 \omega C_i C_v - 2K_{2v}\omega C_v^2 + W_V^-(2)V_2 - D_v C_v k_v^2; \quad (3)$$

$$k_v^2 = Z_{str,v}^a \rho_{str} + 2\pi \sum_{n=2}^{\infty} R_n I_n Z_{Lv}^a(n) + 2\pi \sum_{n=2}^{\infty} R_n V_n Z_{Lv}^a(n);$$

$$W_I^+(n) = W_V^-(n) = 2\pi R_n Z_{Li}^a(n) \bar{D}_i C_i;$$

$$\frac{dC_i}{dt} = (K/\omega) - K_1 \omega C_i C_v - 2K_{2i}\omega C_i^2 + W_I^-(2)I_2 - \bar{D}_i C_i k_i^2; \quad (4)$$

$$k_i^2 = Z_{str,i}^a \rho_{str} + 2\pi \sum_{n=2}^{\infty} R_n I_n Z_{Li}^a(n) + 2\pi \sum_{n=2}^{\infty} R_n V_n Z_{Li}^a(n);$$

$$W_I^-(n) = W_V^+(n) = 2\pi R_n Z_{Lv}^a(n) D_v C_v,$$

where $W_M^+(n)$ – growth rate constant of M-type loops containing n lattice nodes; $W_M^-(n)$ – reduction rate constant of M-type loops containing n lattice nodes; ρ_{str} – the density of dislocation lines (edge) before irradiation; $Z_{str,m}^a$ – the absorption efficiency of m-type PD by a dislocation line; $Z_{Lm}^a(n)$ – the absorption efficiency of m-type PD by a loop containing n lattice nodes. The right part of the equation is a rates of formation of PD (K), their recombination (K_1), formation of a di-cluster from PD of the m-th tyhe (K_{2m}) and disintegration of a di-cluster (V_n – vacancy loop, I_n – interstitial loop), PD absorption by various sinks (k_v^2). Only point defects are mobile, growth or reduction of the loop occurs due to their individual absorption. Thermal evaporation point defects is not taken into account. Only dislocation lines (ρ_{str}) and prismatic loops of both types (V_n; I_n) were taken into account as sinks. Vacancy diffusion is assumed to be isotropic (D_v), the diffusion of SIA is anisotropic ($\bar{D}_i = (D_i^{a^2} D_i^c)^{1/3}$; D_i^a is the SIA diffusion coefficient along the $\langle a \rangle$-axis; D_i^c is the SIA diffusion coefficient along the $\langle c \rangle$-axis); $R_n = \sqrt{n\,\omega/\pi b}$ is a loop radius (a loop of n atoms); $\omega \approx 0.7 \cdot b^3 = 2.33 \cdot 10^{-23}$ cm^3; $b = 3.23 \cdot 10^{-8}$cm is a lattice constant.

Interstitial loops creation begins with di-interstitial creation. Interstitial loops distribution is formed due to point defects absorption by interstitial clusters

$$\frac{dI_2}{dt} = K_{2i}\omega C_i^2 - \left[W_I^+(2) + W_I^-(2)\right] I_2 + W_I^-(3) I_3, \quad (5)$$

$$\frac{dI_n}{dt} = W_I^+(n-1) I_{n-1} - \left[W_I^+(n) + W_I^-(n)\right] I_n + W_I^-(n+1) I_{n+1}. \quad (6)$$

A di-vacancy can form in the system, which initiates a chain of equations for the concentration of V-loops:

$$\frac{dV_2}{dt} = K_{2v}\omega C_v^2 - \left[W_V^+(2) + W_V^-(2)\right] V_2 + W_V^-(3) V_3, \quad (7)$$

$$\frac{dV_n}{dt} = W_V^+(n-1) V_{n-1} - \left[W_V^+(n) + W_V^-(n)\right] V_n + W_V^-(n+1) V_{n+1}. \quad (8)$$

For loops of size $n > 100$ [10], using the Fokker-Planck's differential equation for equations (6) and (8), we write

$$\frac{dI_m}{dt} = \frac{W_I^+(n_{m-1}) I_{m-1} - W_I^+(n_m) I_m}{\Delta x_{m-1}} + \frac{W_I^-(n_{m+1}) I_{m+1} - W_I^-(n_m) I_m}{\Delta x_m}; \quad (9)$$

$$\frac{dV_m}{dt} = \frac{W_V^+(n_{m-1}) V_{m-1} - W_V^+(n_m) V_m}{\Delta x_{m-1}} + \frac{W_V^-(n_{m+1}) V_{m+1} - W_V^-(n_m) V_m}{\Delta x_m}, \quad (10)$$

where each subsequent loop of n – size was determined by the following formula

$$n_1 = 1, \quad n_m = n_{m-1} + \Delta x_m, \quad 2 \le m \le M,$$

$$\Delta x_m = \begin{cases} 1, & 2 \le m \le N, \\ \Delta x_{m-1}\, e^{\varepsilon}, & N < m \le M, \end{cases} \quad \varepsilon = 0.02. \quad (11)$$

RESULTS

Calculations were carried out using the standard LSODA program to $n = 800$, which corresponds to the radius of the loop $R \approx 10^3$ nm. Input date are: $K = 10^{-7}$ dpa$\cdot$s^{-1}; $K_1 = \beta \bar{D}_i = 5.4 \cdot 10^{10}$ s^{-1}; $\beta = 4\pi(r_{iv} / \omega) = 5.4 \cdot 10^{16}$ cm^{-2} is a volume recombination constant; $K_{2m} = 2\beta D_m$; $D_v = 3.0 \cdot 10^{-16}$ cm$^2 \cdot$s^{-1}; $\bar{D}_i = 10^{-6}$ cm$^2 \cdot$s^{-1}; $\rho_{str} = 10^8$ cm^{-2}. The results are presented in Figs. 1, 2.

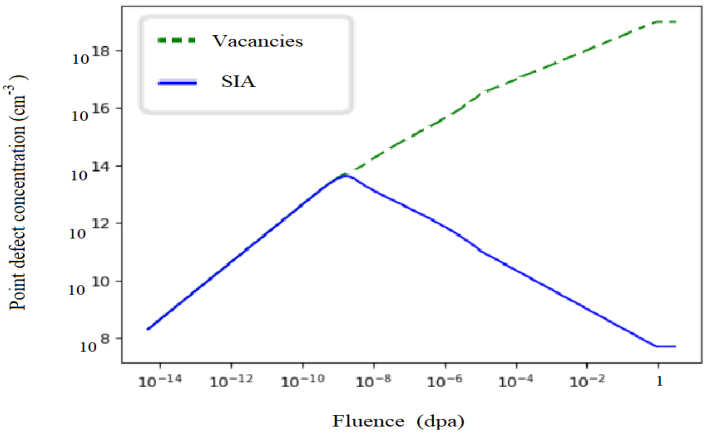

Fig. 1. Variation of point defect concentration on radiation dose: solid line is a self-interstitial atoms, dashed line is a vacancies

As can be seen, point defects concentrations initially grow uniformly. But after $\approx 10^{-8}$ dpa C_i decreases quite sharply, while C_v continues to grow to a constant. It is related to a large difference in the value of point defects diffusion coefficients. SIA are much more mobile and they form prismatic loops earlier, ensuring growth at an early stage of irradiation (see Fig. 2). Vacancies are almost immobile at this stage but due to their relaxation, we have a contraction deformation (ε_c, see Fig. 2).

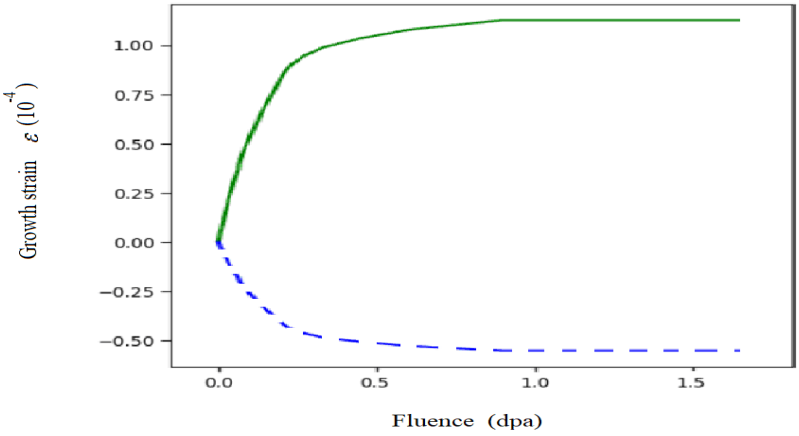

Fig. 2. Variation of deformation on radiation dose: solid line is ε_a, dashed line is ε_c

Fig. 3 shows the distribution of loop sizes calculated by the cluster dynamics model for vacancy and interstitial loops at a dose of 0.1 and 1 dpa for $\bar{D}_i = 10^{-7}$ cm$^2 \cdot$s^{-1}; $\bar{D}_i = 10^{-6}$ cm$^2 \cdot$s^{-1}; $\bar{D}_i = 10^{-5}$ cm$^2 \cdot$s^{-1}; $D_v = 3.0 \cdot 10^{-17}$ cm$^2 \cdot$s^{-1}.

Fig. 3,a,b: dependence of the density of interstitial loops on the radius is non-monotonic. It decreases, reaching a minimum at the loop size of about 10 nm. Then it grows to a maximum and decreases for large sizes. With growth $\bar{D}_i$, the maximum shifts to larger loop sizes. The density of the loops at the maximum decreases with the growth of SIA diffusion coefficient from 10^{11} to 10^9 cm^{-3}. The density of the minimum decreases similarly, from 10^{10} to 10^8 cm^{-3}. For a dose of 1 dpa, the radii of the maxima of interstitial loops are twice as large as for a dose of 0.1 dpa for the corresponding diffusion coefficients.

Fig. 3,c,d: the density of vacancy loops monotonically decreases as their size increases. For a dose of 1 dpa, the sizes of vacancy loops are generally twice as large as for a dose of 0.1 dpa. The increase $\bar{D}_i$ leads to an increase in the average radius of the interstitial loops, which is due to their higher growth rate. On the other hand, the increase $\bar{D}_i$ leads to a significant decrease in their density. Thus, the value $\bar{D}_i$ significantly affects the rate of radiation growth at an early stage (below 1 dpa) due to the growth of interstitial loops. At that time, the changes $\bar{D}_i$ had almost no effect on the size and density of vacancy loops.

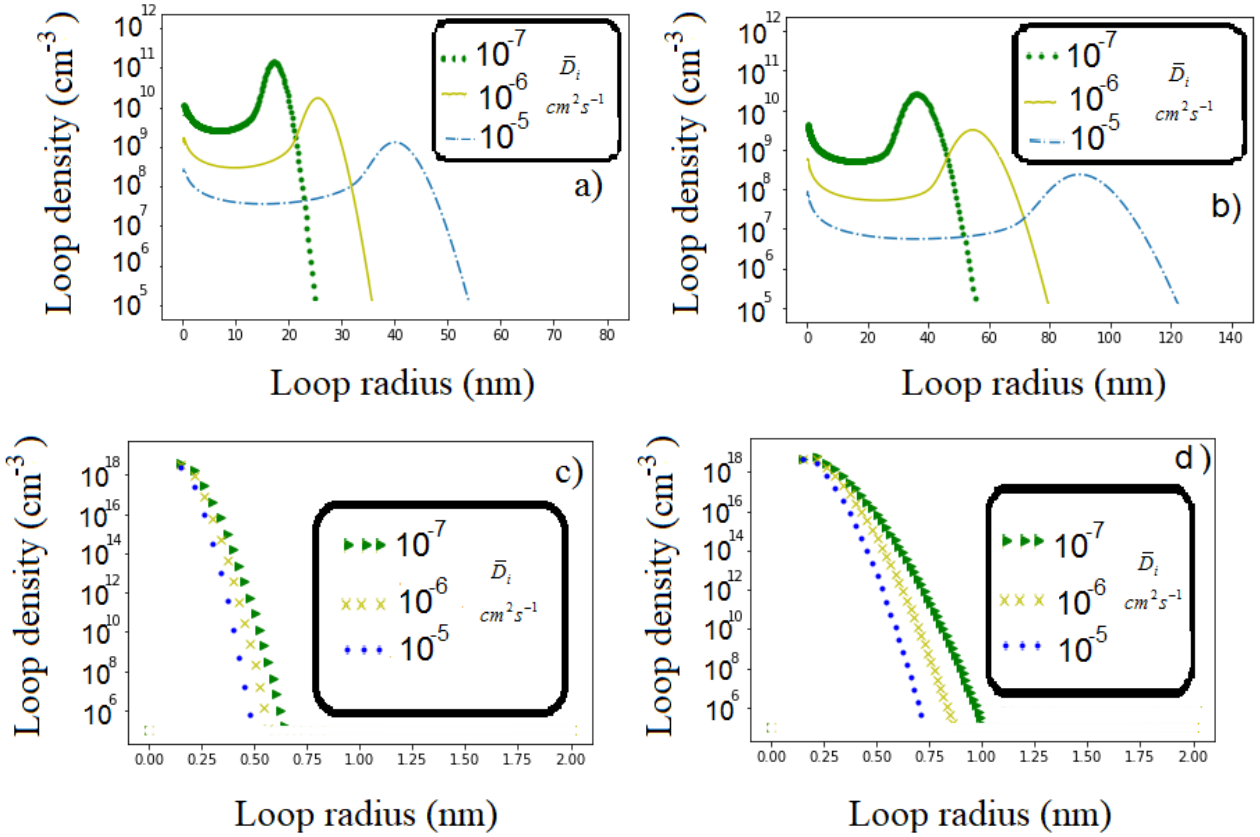

Fig. 3. Dependence of the density of interstitial (a,b) and vacancy (c,d) prismatic loops on their radius for different SIA diffusion coefficients ($\bar{D}_i$) at a dose of 0.1 dpa (a, c) and 1 dpa (b, d) $D_v = 3.0 \cdot 10^{-17}\, cm^2 \cdot s^{-1}$

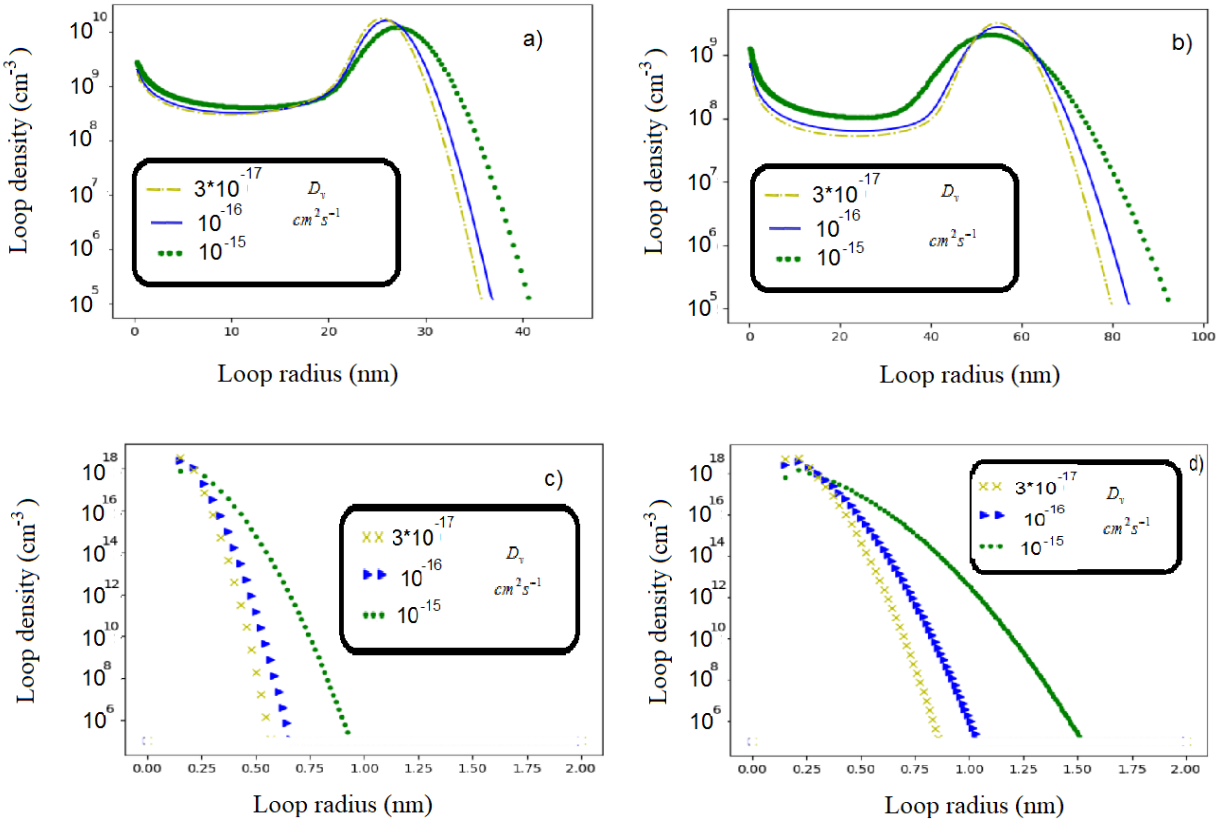

Fig. 4. Dependence of the density of interstitial (a, b) and vacancy (c, d) prismatic loops on their radius for different vacancy diffusion coefficients (D_v) at a dose of 0.1 dpa (a, c) and 1 dpa (b, d) $\bar{D}_i = 10^{-6}\, cm^2 \cdot s^{-1}$

Fig. 4 shows the dependence of the density of interstitial and vacancy loops on the radius at a dose of 0.1 and 1 dpa for $D_v = 3 \cdot 10^{-17}\,\mathrm{cm}^2 \cdot \mathrm{s}^{-1}$; $D_v = 10^{-16}\,\mathrm{cm}^2 \cdot \mathrm{s}^{-1}$; $D_v = 10^{-15}\,\mathrm{cm}^2 \cdot \mathrm{s}^{-1}$; $\bar{D}_i = 10^{-6}\,\mathrm{cm}^2 \cdot \mathrm{s}^{-1}$.

As can be seen from Fig. 4,a,b the density and size of interstitial loops practically do not change when the vacancy diffusion coefficient changes. With growth D_v only for loops of large size a slight increase in their density is observed. The density of vacancy loops increases with growth D_v (see Fig. 4,c,d).

If we look at the loop size distribution calculated by the Cluster Dynamics Model for vacancy and interstitial loops, we observe (see Figs. 3, 4) that at an early stage interstitial loops grow whereas vacancy clusters of significant sizes are practically not formed (only very small vacancy clusters are predicted by the model). This growth of interstitial prismatic loops is the reason for the elongation of the crystals along the *a*-axis to 1 dpa, while the contraction along the c-axis is due to the relaxation of vacancies. At the beginning of irradiation, prismatic dislocation loops absorb much more SIA than vacancies, since $\bar{D}_i C_i >> D_v C_v$ ($C_i \approx C_v$ and $\bar{D}_i >> D_v$), which corresponds to the rapid growth of interstitial loops. Then the vacancy concentration increases until $D_v C_v$ it approaches $\bar{D}_i C_i$. As a consequence, interstitial prismatic dislocation loops absorb more and more vacancies, which makes the growth rate lower and lower. In the permanent regime (above 1 dpa), prismatic dislocation loops absorb so many vacancies as SIA and the crystals do not grow any longer (see Figs. 1, 2).

The studied effects of radiation growth can also be used to explain the changes in mechanical characteristics observed during simulation modeling of the behavior of zirconium alloys under the influence of nuclear fuel fission fragments [11].

SUMMARY

1. The dependence of point defects concentration was calculated on the dose in the absence of thermal radiation

2. The dependences of interstitial and vacancy loops concentration on their radius were obtained for doses of 0.1 dpa and 1 dpa and different diffusion coefficients.

– The density and size of vacancy loops increase with growth D_v. Changes in vacancies diffusion coefficient almost did not affect the size and density of interstitial loops.

– $\bar{D}_i$ affects the growth rate of internodal loops during the early stage of “irradiation growth” of a zirconium single crystal. (below 1 dpa). Changes in SIA diffusion coefficient almost did not affect the size and density of vacancy loops.

3. The dependence of growth deformation along the main axes of single crystal $\langle a \rangle$ and $\langle c \rangle$ was obtained

REFERENCES

1. M. Griffiths, M.H. Loretto, R.E. Sallmann. Electron damage in zirconium: I. defect structure and loop character // *J. Nucl. Mater*. 1983, v. 115, p. 313.

2. M. Griffiths, M.H. Loretto, R.E. Sallmann. Electron damage in zirconium: II. Nucleation and growth of c-component loops // *J. Nucl. Mater*. 1983, v. 115, p. 323.

3. M. Griffiths, M.H. Loretto, R.E. Sallmann. Anisotropic distribution of dislocation loops in HVEM-irradiated Zr // *Philos. Mag. A*. 1984, v. 49, p. 613.

4. M. Griffiths. A review of microstructure evolution in zirconium alloys during irradiation // *J. Nucl. Mater*. 1988, v. 159, p. 190.

5. M.R. Hayns. The nucleation and early growth of interstitial dislocation loops in irradiated materials // *J. Nucl. Mater.* 1975, v. 56, p. 267.

6. L.K. Mansur. Theory and experimental background on dimensional changes in irradiated alloys. // *J. Nucl. Mater.* 1994, v. 216,p. 97.

7. R Bullough, M.H. Wood. Mechanisms of radiation induced creep and growth // *Journal of Nuclear Materials.* 1980, v. 90. p. 1-21.

8. O. Le Bacq, F. Willaime. Unrelaxed vacancy formation energies in group-IV elements calculated by the full-potential linear muffin-tin orbital method: Invariance with crystal structure // *Phys. Rev. B.* 1999, v. 59, p. 8508.

9. F. Christien, A. Barbu. Cluster Dynamics modelling of irradiation growth of zirconium single crystals // *Journal of Nuclear Materials*. 2009, v. 39, p. 153-161.

10. А.А. Туркін. *Теорія фазових перетворень у неупорядкованих сплавах заміщення під опроміненням*: Дис. …. д-ра фіз.-мат. наук. Харків, 2010, 309 с.

11. V.F. Klepikov, V.V. Lytvynenko, Yu.F. Lonin, A.G. Ponomarev, O.A. Startsev, V.T. Uvarov. Behavior of Zr1%Nb Alloy under Swift Kr ion and Intense Electron Irradiation // *Journal of Nano- and Electronic Physics*. 2015, v. 7, N 4, p. 04016 (7 p.).

Article received 30.12.2025

МОДЕЛЮВАННЯ РАННЬОЇ СТАДІЇ ЯВИЩА РАДІАЦІЙНОГО РОСТУ ЦИРКОНІЮ

О.Г. Троценко*, *П.М. Остапчук

Метод кластерної динаміки був використаний для опису ранньої стадії «радіаційного росту» монокристалу цирконію, що дозволяє описати еволюцію його мікроструктури з дозою опромінення. Наведено результати чисельних розрахунків залежності концентрації точкових дефектів від дози за умови відсутності теплового випромінювання, залежності деформації росту вздовж головних осей монокристалу $\langle a \rangle$, $\langle c \rangle$ і залежності концентрації міжвузельних і вакансійних петель від їх радіуса для доз до 1 зна і різних коефіцієнтів дифузії точкових дефектів.